Supporting Information for Quantification and Classification of Engineered, Incidental, and Natural Cerium-Containing Particles by spICP-TOFMS

Sarah Szakas[1], Richard Lancaster[1], Ralf Kaegi[2], Alexander Gundlach-Graham[1*]

1. Department of Chemistry, Iowa State University, Ames, Iowa
2. Eawag, Dubendorf, Switzerland

Table of Contents

Table S1 describes the sampling scheme for mixtures used in experiment one, in which ratios of anthropogenic-NPs:NNPs were investigated. The volume of each stock suspension used was based on the classified particle PNCs. In total, seven samples were used for each analysis of the high and low Ce-NNP backgrounds.

Experiment Set One – Anthropogenic-NP: NNP			
Stock PNC (particles mL^{-1})			
	Ce-NNP	Ce-INP	Ce-ENP
	5.1×10^{6}	8.9×10^{5}	1.3×10^{7}
Total Vol (mL)	Dilution Factors of Ce-NP Stocks		
15	High Background 138 Low Background 1360	5000	15000
15		3000	15000
15		1500	15000
15		500	7500
15		300	3000
15		58	700
15		12	135
Predicted Ce-ENP:Ce-NNP		**Predicted Ce-INP:Ce-NNP**	
High Ce-NNP background	Low Ce-NNP background	High Ce-NNP background	Low Ce-NNP background
1:42	1:4	1:207	1:20
1:42	1:4	1:124	1:12
1:42	1:4	1:62	1:6
1:19	1:2	1:20	1:2
1:9	1:1	1:12	1:1
1:2	5:1	1:2	4:1
3:1	26:1	2:1	20:1
5:1	50:1	4:1	40:1

Table S2 describes the sampling scheme for mixtures in experiment two, where one anthropogenic-NP's PNC was altered across five samples while the other anthropogenic-NP's PNC stayed constant. Each sample contained the same spiked amount of NNPs (to obtain the same PNC) across 10 samples. For each anthropogenic-NP, there are five dilutions of the stock suspension. Replicate dilutions correspond to a different dilution of the other anthropogenic-NP.

Experiment Set Two – Classification of all Ce-NPs in varying PNCs				
		Stock PNC (particles mL^{-1})		
		Ce-INP	Ce-ENP	Ce-NNP
		5.9×10^{6}	2.7×10^{6}	1.9×10^{7}
	Sample	**Dilution Factors of Ce-NP Stocks**		
Fig. 8a	1	1000	1000	300
	2	1000	500	
	3	1000	250	
	4	1000	50	
	5	1000	10	
Fig. 8b	6	1000	1000	
	7	500	1000	
	8	250	1000	
	9	100	1000	
	10	50	1000	

Table S3 Instrument and calibration parameters

	Droplets	*Curve*
Spray Chamber	Baffled cyclonic quartz	Perkin Elmer Baffled Cyclonic quartz
Nebulizer	PFA PrepFAST	
Nebulizer *(l min^{-1})*	0.87	1.01
Auxiliary gas *(l min^{-1})*	1.00	0.80
Cool gas *(l min^{-1})*	14	
RF power *(W)*	1550	
Add. Gas Ar/He *(l min^{-1})*	7.5x10^{-3}/0.26	n/a
Transport Efficiency (%)	14	20
Notch filter (m/z)	17.2, 29.0, 36.5, 40.0	17.3, 28.5, 38.0, 40.5

Table S4: Isotopes Used

Element	*Isotopes Used*
Y	^{89}Y
Cs	^{133}Cs
La	^{139}La
Ce	^{140}Ce
Pr	^{141}Pr
Nd	^{144}Nd, ^{146}Nd
Gd	^{157}Gd
Sm	^{147}Sm, ^{149}Sm
Th	^{232}Th
U	^{238}U

Table S5: Calibration Standards and Concentrations

Droplets (ng mL^{-1})		Standard Curve (ng mL^{-1})					Detection Efficiency (cts g^{-1})
Ce	10.18	0.49	1.00	10.07	50.51	0.49	5.09E+17
Fe	52.02	2.51	5.11	51.47	258.14	2.51	2.61E+15
La	10.49	0.51	1.03	10.38	52.04	0.51	4.85E+17
Nd	10.38	0.50	1.02	10.27	51.53	0.50	4.09E+17
Pr	10.80	0.52	1.06	10.68	53.57	0.52	5.95E+17
Th	10.38	0.50	1.02	10.27	51.53	0.50	1.01E+18
U	10.59	0.51	1.04	10.48	52.55	0.51	1.01E+18
Y	12.03	0.58	1.18	11.90	59.69	0.58	1.84E+17
Cs	9.50						
Cs Uptake	0.97						

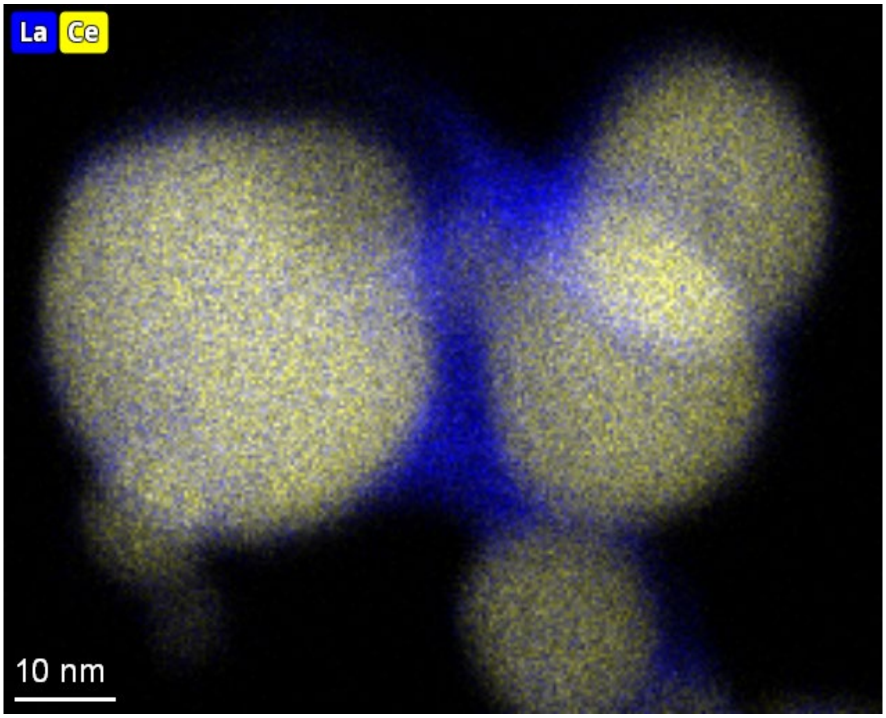

Fig S1 Elemental distribution map of Ce (yellow) and La (blue) in Ce-INPs documenting the presence of Ce and La -rich phases. The elemental distributions map indicates considerable variability of Ce and La abundances within individual particles; however, spICP-TOFMS demonstrates these ratios are more conserved in the analysis of entire particles.

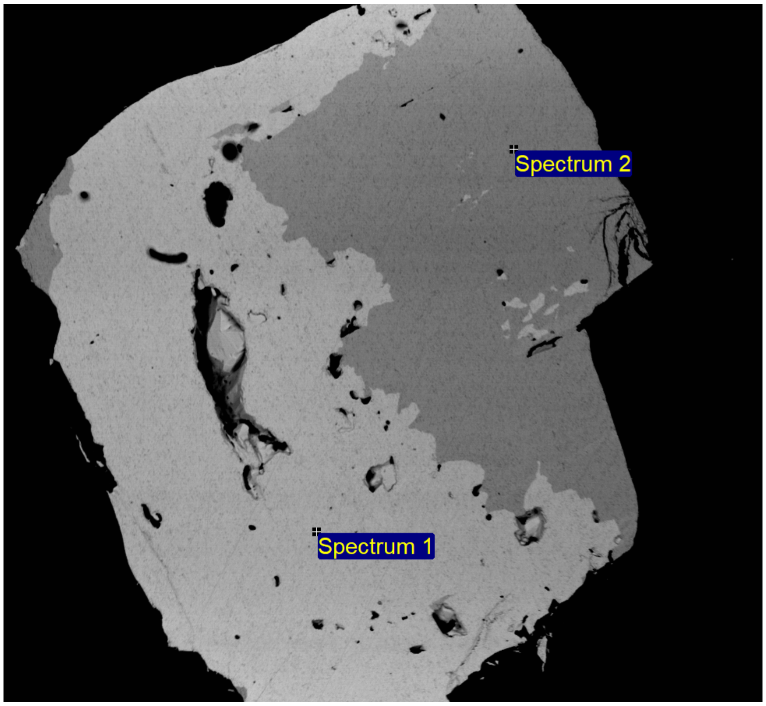

Element	Spectrum 1	Spectrum 2
Al	1.3	2.0
Si	0.9	1.1
Ca	**0.2**	**10.7**
La	**8.6**	**5.8**
Ce	**18.2**	**13.1**
Pr	2.0	1.8
Nd	7.2	5.8
Sm	0.9	0.9
Eu	0.2	0.3
Gd	0.3	0.3
O	60.2	58.1

Fig. S2 Backscattered electron (BSE) image of a polished resin embedded mineral grain, extracted from a host rock. The sample was investigated on a scanning electron microscope (NanoSEM230, FEI). The quantified elemental contents are given to the right (in atomic weight %). Due to the strong overlap of the x-ray L-lines of the REEs, the quantified abundances need to be treated with care. Nevertheless, the contrasting contents of Ca are obvious, allowing distinction and detection of both bastnaesite and parisite.

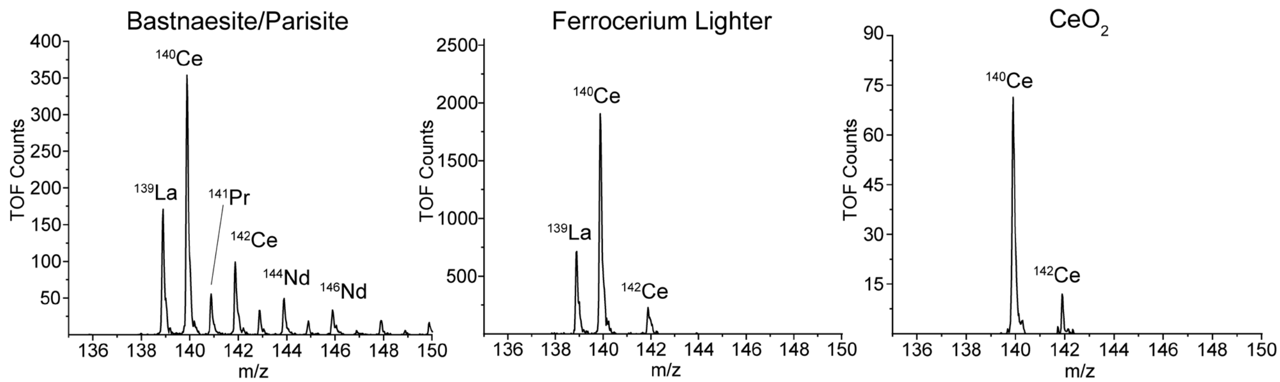

Fig. S3 Mass spectra of single particles for each NP type zoomed in on *m/z* values 135-150.

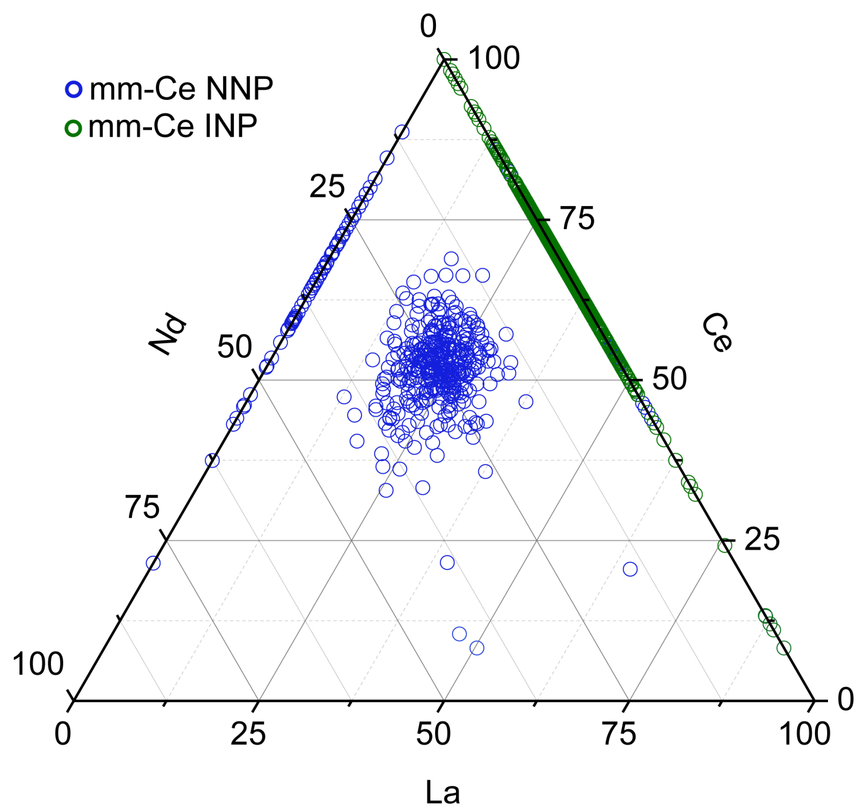

Fig. S4 Multi-metal NPs from both Ce-NNPs and Ce-INPs are plotted together on three axes to illustrate relative REE compositions of each particle. There is no detectable Nd found in the Ce-INPs (green), so they are all located along the right side, on the Ce axis. The majority of Ce-NNPs (blue) are composed of all three elements and are seen clustered in the center of the diagram, and a few Ce-NNPs without La, are plotted on the left, Nd axis.

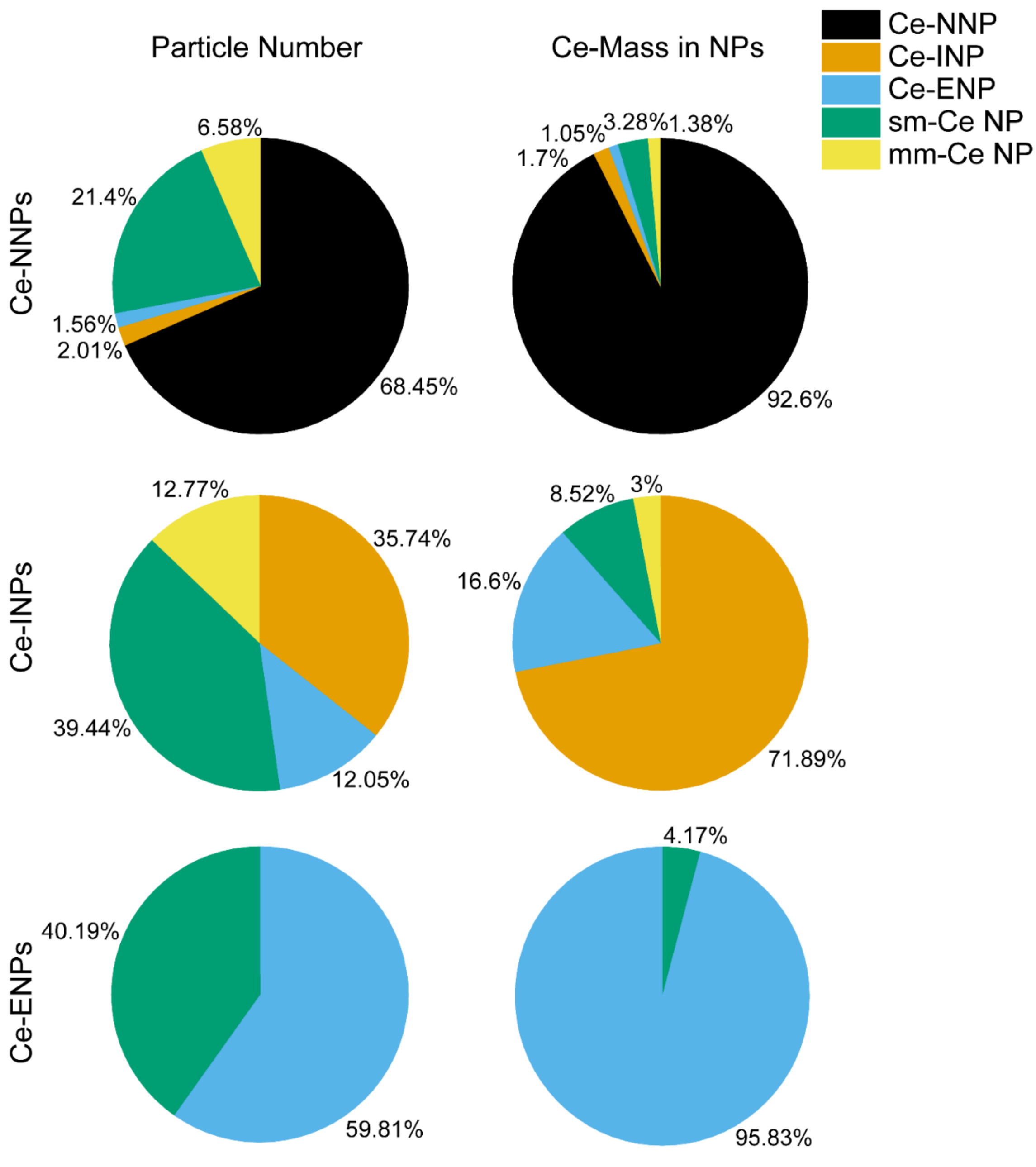

Fig. S5 Pie charts showing the percent recovery in terms of particle number (left) and cerium mass (right) for classification of the stock suspensions of Ce-NNPs, Ce-INPs, and Ce-ENPs. Ce-NP events with signals lower than particle-type detection limits ($L_{D,sp,Ce,Ce\text{-}La}$ or $L_{D,sp,Ce,Ce\text{-}Nd}$) are reported as unclassified. Unclassified particles are true Ce-NP events and are included in the determination of total Ce-NP concentrations but are too small for further classification. Percent recoveries in terms of Ce mass are higher than number-based recoveries because particles with more mass (i.e. larger size) are more readily classified than small particles.

Table S6 Approximate minimum particle diameters for classification were calculated using the Ce-NNP ratios for Ce:La and Ce:Nd. Estimations assume spherical shape of particles. Densities of each particle type were estimated through stoichiometry of the natural minerals, CeO_2, and ferrocerium composition. Each particle type diameter was estimated using the mass of Ce at $L_{D,sp,Ce,Ce\text{-}Nd}$ and repeated using the $L_{c,sp,Ce}$ to approximate the lowest-size particle detectable. $L_{D,sp,Ce,Ce\text{-}Nd}$ was higher, and therefore chosen over $L_{D,sp,Ce,Ce\text{-}La}$, and the mass of Ce at the L_D value was 96.1 ag.

NP type	Density (g cm^{-3})	Diameter (nm) to classify	Diameter (nm) using $L_{c,sp,Ce}$
Ce-ENP *CeO_2*	7.2	31.5	21.5
Ce-INP *$CeLa_{0.8}Fe_{0.2}$*	6.5	34.9	23.9
Ce-NNP *$(Ce,La,Nd)CO_3F$*	5.0	44.8	30.6

Table S7 We explore a range of confidence intervals (90% to 99%) below to set $L_{D,sp,Ce,Ce\text{-}La}$ and $L_{D,sp,Ce,Ce\text{-}Nd}$ values. Increasing our confidence interval (or decreasing β) forces the L_C to be set farther away from the mean (λ) count distribution. Since the L_C value remains unchanged for any CI, the L_D determined must account for the CI chosen. This means a higher CI results in a higher L_D. The element ratios remain constant, so the detection limit in counts of Ce will also be elevated. As we increase the CI, we increase accuracy in classifying particles (less false-positives), but we increase false-negative, or unclassified, determinations.

Ce-NNP Stock	**90% CI**	**95% CI**	**99% CI**
$\boldsymbol{L_{D,sp,Ce,Ce-La}}$	44.5	48.6	57
$\boldsymbol{L_{D,sp,Ce,Ce-Nd}}$	49.8	54.4	64.2

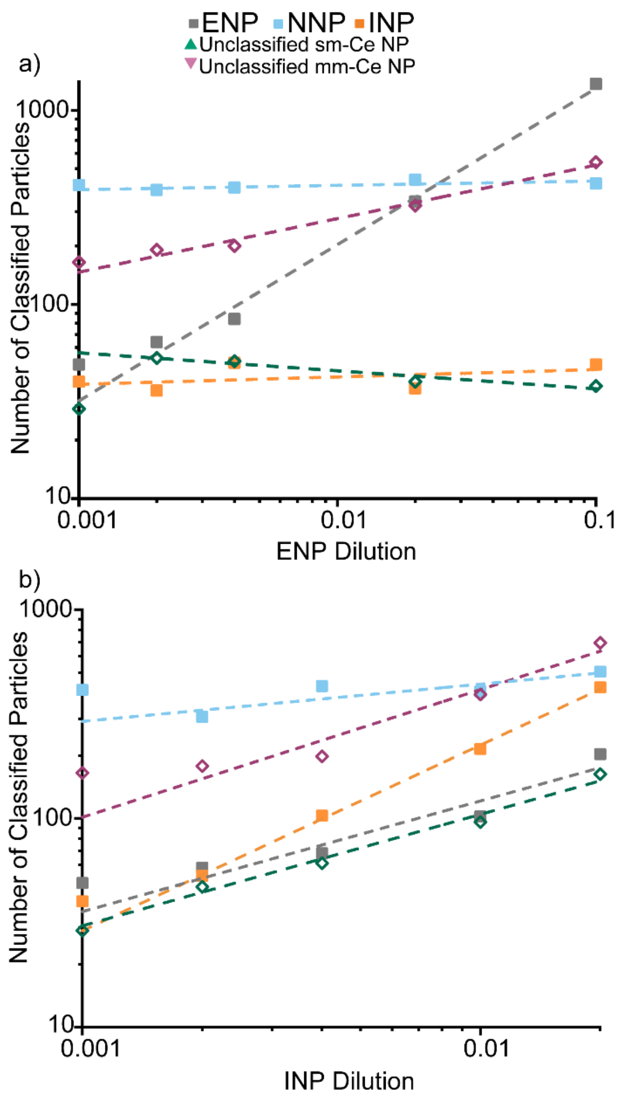

Fig. S6 The data from Fig. 8 is replotted along with unclassified particles. As Ce-INPs increase in PNC, there is an increase in the number of unclassifiable sm-Ce NPs as well as mm-Ce NPs. This is expected because Ce-INPs have heterogeneous Ce:La ratios, as well as higher background counts of Ce and La. More NPs are classified as either Ce-only, hence the increase in unclassifiable sm-Ce NPs as well as Ce-ENPs. Unclassified mm-Ce NPs arise from particles that have detectable La, but not enough counts of Ce to distinguish whether it is a Ce-INP or Ce-NNP.

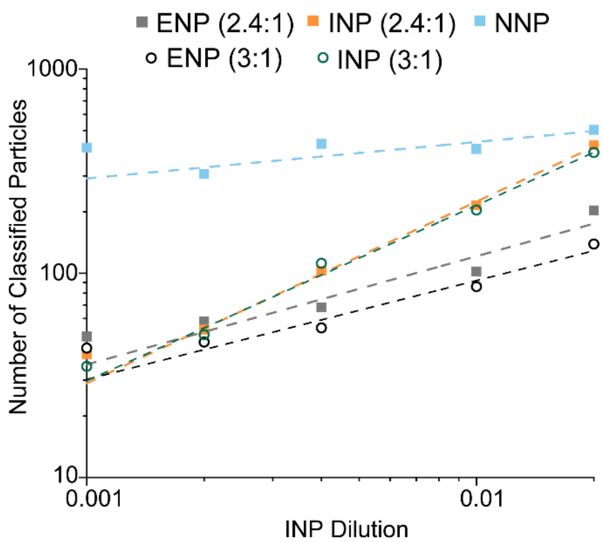

Fig. S7 The classification of ENPs is shown as the ratio of Ce:La ($R_{Ce:La}$) is increased. Due to the heterogeneity of the Ce:La ratio in Ce-INPs, increasing the Ce:La ratio from 2.4:1 (orange) to 3:1 (green) helps to decrease the amount of false-positive Ce-ENPs at higher Ce-INP PNCs. At either ratio shown, Ce-INPs remained relatively unchanged. While this approach limits false-Ce-ENPs, some particles are still false positive classifications.

Table S8 Mass ratios are given for Ce:La and Ce:Nd in the Ce-minerals allanite, monazite, and bastnaesite/parisite and for two types of ferrocerium lighters (disposable lighter and striker). Mass ratios were obtained by linear least squares fitting of the masses of Ce, La, and Nd collected from individual particles, as done previously with the bastnaesite/parisite and lighter particle data.

Mineral	**Ce:La mass ratio**	**Ce:Nd mass ratio**
Allanite	2.5:1	1.2:1
Bastnaesite/Parisite	2.3:1	2.3:1
Monazite	3.3:1	1.4:1
Disposable Lighter	2.3:1	n/a
Bernzomatic	1.9:1	n/a

Table S9 The table below shows the absolute difference in the number of classified particles from the particle-type specific detection limits used in the paper with Poisson-Normal approximations, and the detection limits determined by a Monte Carlo simulation in which lambda of Poisson-distributed data was iteratively increased until 95% of the distribution was above the critical value. Samples 1-10 relate to the second set of experiments, shown in Table S2. For all cases, we classify more particles with the Poisson-Normal detection-limit thresholds because the Poisson-Normal approximation slightly underestimates variance of the TOFMS data. In parenthesis, we also report the percent difference of the number of particles classified using the Poisson-Normal approximation and the Monte-Carlo-determined Poisson $L_{D,sp}$ values.

	Sample	Ce-NNPs	Ce-INPs	Ce-ENPs
Fig. 8a	1	0	1 (2.4%)	0
	2	0	1 (2.7%)	1 (1.4%)
	3	0	1 (1.9%)	2 (2.3%)
	4	0	3 (7.6%)	4 (1.1%)
	5	0	5 (9.7%)	23 (1.6%)
Fig. 8b	6	0	1 (2.4%)	0
	7	0	2 (3.7%)	1 (1.7%)
	8	0	1 (0.9%)	3 (4.4%)
	9	0	2 (0.9%)	2 (1.9%)
	10	0	5 (1.1%)	6 (3.0%)

Table S10 The background of each sample run in this manuscript is given below, in ng mL^{-1}. The average distribution of the Ce background counts from a water blank was subtracted from the Ce background of each sample. Using detection efficiency, as well as the length of the run, the total grams of Ce from the background was calculated. This total Ce-mass was then divided by the total volume of sample put into the plasma. Dissolved concentration results for experiment one, two and the stocks are below. Both experiments are ordered from least to most concentrated sampled (left to right).

Experiment 1							
Low Ce-NNP bkgd	0.15	0.15	0.20	0.26	1.57	2.76	3.54
High Ce-NNP bkgd	0.47	0.50	0.52	0.56	0.73	1.61	7.24
Experiment 2							
Ce-ENP Increasing	0.16	0.13	0.11	0.15	0.13		
Ce-INP Increasing	0.16	0.14	0.17	0.24	0.39		
Stock Particle Suspensions							
Ce-NNP (300x)	0.079						
Ce-ENP (100x)	0.002						
Ce-INP (100x)	0.055						

Table S11 Particle coincidence has been estimated via Poisson statistics and number of particle events measured per sample. All samples were kept to percent coincidence events below 5%. Coincidence of two particles being detected in the same time bin includes particles of the same type as well as two different particle types. Estimations given are only for single metal and multi-metal particles with elements Ce, La, Nd, Pr, and Th.

Experiment 1		Experiment 2	
Low Ce-NNP background	High Ce-NNP background	Low to High Ce-ENP PNC	Low to High Ce-INP PNC
<1%	<1%	<1%	<1%
<1%	<1%	<1%	<1%
<1%	<1%	<1%	<1%
<1%	<1%	<2%	<2%
<1%	<1%	<3%	<3%
<1%	<1%		
<2%	<2%		